THERMAL DISPERSION TENSOR IN A POROUS MEDIA MODELED AS INFINITE ARRAYS OF LONGITUDINALLY AND TRANSVERSALLY-DISPLACED ELLIPTIC RODS

Marcos Heinzelmann Junqueira Pedras
Instituto de Pesquisa e Desenvolvimento IP&D, UNIVAP
12244-000, São José dos Campos, SP, Brasil. E-mail: pedras@univap.br

Marcelo J.S. De-Lemos*
Departamento de Energia - IEME
Instituto Tecnológico de Aeronáutica - ITA
12228-900 - São José dos Campos - SP – Brasil
E-mail: delemos@mec.ita.br
* Corresponding author

Abstract. *Thermal dispersion in porous media is an import phenomenon in combustion and in steam injection systems for Enhanced Oil Recovery methods. Accordingly, the study of flow through porous media has gained much attention lately and advances in proper modeling of such flows, which includes non-linear effects, have been published. In this work, the results of thermal dispersion tensors calculations for two porous media with distinct morphologies, one formed by a spatially periodic array of longitudinally-displaced elliptic rods and the other with transversally-displaced elliptic rods, are presented and discussed. For the sake of simplicity, just one unit-cell, together with periodic boundary conditions for mass and momentum equations, and Neumann and Dirichlet conditions for the temperature equation, was used to represent such media. The numerical methodology herein employed is based on the control-volume approach. Turbulence is assumed to exist within the fluid phase and high and low Reynolds k-e models are used to model such non-linear effects. The flow equations at the pore-scale were numerically solved using the SIMPLE method on a non-orthogonal boundary-fitted coordinate system.*

Keywords: *porous media, thermal dispersion, periodic boundary conditions, low Reynolds k-e model, macroscopic energy equation.*

1. Introduction

Due to its great application in the industry and science, the study of the flow in porous media has received great attention lately and advances in proper modeling of such flows, including non-linear effects, have been published (Pedras and de Lemos, 2001a; de Lemos and Pedras, 2001; Rocamora and de Lemos, 2000; Pedras and de Lemos, 2001b; Pedras and de Lemos, 2001c; Pedras *et al.*, 2003a; Pedras *et al.*, 2003b; Pedras and de Lemos, 2003). Engineering systems based on fluidized bed combustion, enhanced oil reservoir recovery, combustion in an inert porous matrix, underground spreading of chemical waste and chemical catalytic reactors are just a few examples of such applications. In some of these applications the thermal dispersion in porous media is an

important phenomenon, in which one has used (Hsu and Cheng, 1990; Kaviany, 1995; Ochoa-Tapia and Whitaker, 1997; Moyne, 1997; Quintard *et al.*, 1997; Kuwahara and Nakayama, 1998; Nakayama and Kuwahara, 1999) the notion of a Representative Elementary Volume (REV, Fig. 1) for the mathematical treatment of governing equations. These models, based on the macroscopic point of view, lose details on the flow pattern inside the REV and, together with ad-hoc information, provide global flow properties such as average velocities and temperatures.

Such flows can also be analyzed by modeling the topology of the porous medium and resolving the flow equations at the pore-scale. This treatment reveals the flow structure at the pore-scale level and was used by (Quintard *et al.*, 1997; Kuwahara and Nakayama, 1998; Nakayama and Kuwahara, 1999; Rocamora and de Lemos, 2002) to calculate the thermal dispersion tensors with periodic boundary condition for the mass, momentum and the energy equations.

The aim of this work is to present the thermal dispersion calculations results obtained for two porous media, one formed by a spatially periodic array of longitudinally-displaced elliptic rods and the other with transversally-displaced elliptic rods. The motivation of the use of these two types of porous media is that they spanning from a low-drag porous media, driven principally by viscous drag (longitudinal ellipses), to high-drag porous media, driven principally by form drag (transverse ellipses), Pedras and de Lemos (2003).

For the sake of simplicity, just one unit-cell, together with periodic boundary conditions for mass and momentum equations, and Neumann and Dirichlet conditions for the temperature equation, was used to represent such media. Turbulence is assumed to exist within the fluid phase and high and low Reynolds *k-e* models are used to model such non-linear effects.

The flow equations at the pore-scale were numerically solved using the SIMPLE method on a non-orthogonal boundary-fitted coordinate system. The integrated results were compared to the existing data presented in the literature.

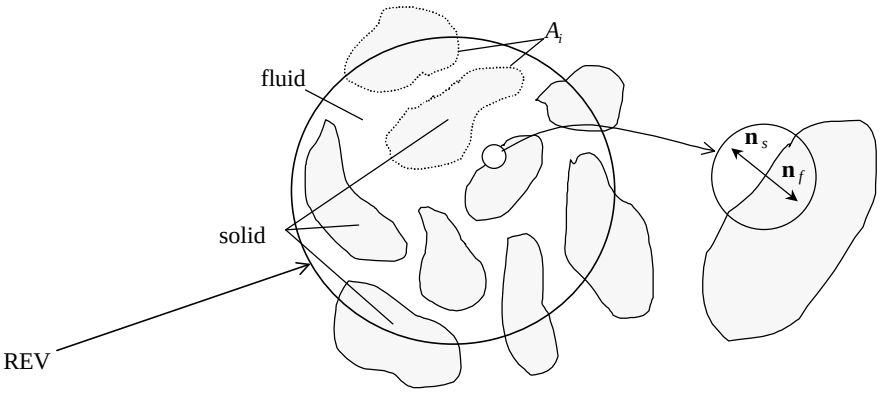

Figure 1. Representative elementary volume (REV).

2. Microscopic Equations

The following microscopic transport equations describe the flow field and the heat transfer process within a porous medium, where barred quantities represent time-averaged components and primes indicate turbulent fluctuations:

Fluid Phase (incompressible fluid):

$$\nabla \cdot \overline{\mathbf{u}} = 0 \tag{1}$$

$$r_f[\frac{\partial \overline{\mathbf{u}}}{\partial t} + \nabla \cdot (\overline{\mathbf{u}}\,\overline{\mathbf{u}})] = -\nabla \overline{p} + \nabla \cdot \{m[\nabla \overline{\mathbf{u}} + (\nabla \overline{\mathbf{u}})^T] - r_f \overline{\mathbf{u}'\mathbf{u}'}\} \tag{2}$$

$$r_f c_{pf}[\frac{\partial \overline{T}_f}{\partial t} + \nabla \cdot (\overline{\mathbf{u}}\,\overline{T}_f)] = \nabla \cdot [k_f \nabla \overline{T}_f - r_f c_{pf} \overline{\mathbf{u}'T_f'}] \tag{3}$$

$$r_f[\frac{\partial k}{\partial t} + \nabla \cdot (\overline{\mathbf{u}}k)] = \nabla \cdot [(m + \frac{m_t}{s_k})\nabla k] - r_f \overline{\mathbf{u}'\mathbf{u}'} : \nabla \overline{\mathbf{u}} - r_f e \tag{4}$$

$$r_f[\frac{\partial e}{\partial t} + \nabla \cdot (\overline{\mathbf{u}}e)] = \nabla \cdot [(m + \frac{m_t}{s_e})\nabla e] + [C_1(-r_f \overline{\mathbf{u}'\mathbf{u}'} : \nabla \overline{\mathbf{u}}) - C_2 f_2 r_f e]\frac{e}{k} \tag{5}$$

$$- r_f \overline{\mathbf{u}'\mathbf{u}'} = m_t[\nabla \overline{\mathbf{u}} + (\nabla \overline{\mathbf{u}})^T] - \frac{2}{3} r_f k \mathbf{I} \tag{6}$$

$$- r_f c_{pf} \overline{\mathbf{u}'T_f'} = r_f c_{pf} \frac{n_t}{s_t} \nabla \overline{T}_f \tag{7}$$

$$m_t = r_f n_t = r_f C_m f_m \frac{k^2}{e} \tag{8}$$

Solid Phase:

$$r_s c_{ps} \frac{\partial \overline{T}_s}{\partial t} = \nabla \cdot [k_s \nabla \overline{T}_s] \tag{9}$$

where $\mathbf{u}$ is the microscopic velocity, r_f and r_s the fluid and solid densities, p the thermodynamic pressure, m and m_t the dynamic and turbulent viscosities, T_f and T_s the fluid and solid temperatures, c_{pf} and c_{ps} the fluid and solid specific heat at constant pressure, k_f and k_s the fluid and solid thermal conductivities, k the turbulent kinetic energy and e the dissipation of k. In the equations s_k, s_e and s_t are effective Prandtl numbers, C_1, C_2 and C_m are dimensionless constants and f_2 and f_m damping functions.

In this work the use of the low Re *k-e* model is justified by the fact that the turbulent flow in porous media occurs for Reynolds numbers (based on the pore) relatively low. To account for the low Reynolds effects, the following damping functions and model constants were adopted (Abe *et al.*, 1992):

$$f_2 = \left\{1 - \exp\left[-\frac{(ne)^{0.25} n}{3.1n}\right]\right\}^2 \times \left\{1 - 0.3\exp\left[-\left(\frac{(k^2/ne)}{6.5}\right)^2\right]\right\} \tag{10}$$

$$f_m = \left\{1 - \exp\left[-\frac{(ne)^{0.25} n}{14n}\right]\right\}^2 \times \left\{1 + \frac{5}{(k^2/ne)^{0.75}}\exp\left[-\left(\frac{(k^2/ne)}{200}\right)^2\right]\right\} \tag{11}$$

$$C_m = 0.09\,,\ C_1 = 1.5\,,\ C_2 = 1.9\,,\ s_k = 1.4\,,\ s_e = 1.3\,. \tag{12}$$

While for the high Re *k-e* model it was used the standard constants of Launder and Spalding (1974).

For the unit-cell represented in Fig. (2) and with the assumption of macroscopic fully developed uni-dimensional flow, the boundary conditions utilized are given as follow:

at the walls, $\overline{\mathbf{u}} = 0$; $\overline{T}_f = \overline{T}_s$; $\mathbf{n}_f \cdot (k_f \nabla \overline{T}_f) = -\mathbf{n}_s \cdot (k_s \nabla \overline{T}_s)$; $k = 0$ and $e = n \frac{\partial^2 k}{\partial n^2}$, (13)

on $x = 0$ and $x = H$ periodic boundaries (momentum equation),

$$\bar{u}\big|_{x=0} = \bar{u}\big|_{x=H},\ \bar{v}\big|_{x=0} = \bar{v}\big|_{x=H},\ k\big|_{x=0} = k\big|_{x=H} \text{ and } e\big|_{x=0} = e\big|_{x=H} \tag{14}$$

on $y = 0$ and $y = H$,

$$\frac{\partial \bar{u}}{\partial y} = \frac{\partial \bar{v}}{\partial y} = \frac{\partial k}{\partial y} = \frac{\partial e}{\partial y} = 0 \tag{15}$$

where n_f and n_s are the coordinates normal to the interface (Fig. 1) and u and v the components of $\mathbf{u}$.

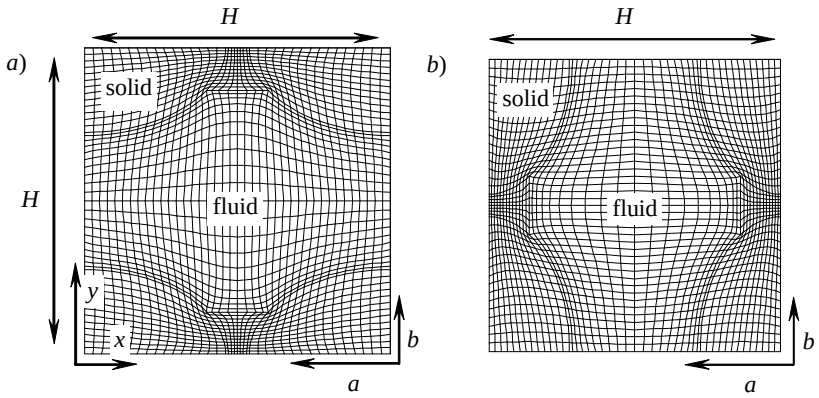

Figure 2. Unit-cell: *a*) longitudinal-elliptic rods ($a/b = 5/3$) and *b*) transverse-elliptic rods ($a/b = 3/5$).

The temperature boundary conditions will be presented in the next section.

3. Thermal Dispersion Modeling

Using the double decomposition concept (Pedras and de Lemos, 2001a) of a general quantity j_b in the b phase,

$$j_b = \langle \bar{j}_b \rangle^b + {}^i\bar{j}_b + \langle j'_b \rangle^b + {}^i j'_b \tag{16}$$

and following the procedure of Rocamora and de Lemos (2000) and Rocamora and de Lemos (2002), the volume averaging of the energy equations (3) and (9) over the REV, assuming local thermal equilibrium between the solid and fluid phases, namely $\langle \bar{T}_f \rangle^f = \langle \bar{T}_s \rangle^s = \langle \bar{T} \rangle$, renders:

$$[f_f \rho_f c_{pf} + f_s \rho_s c_{ps}] \frac{\partial \langle \bar{T} \rangle}{\partial t} + \rho_f c_{pf} \nabla \cdot (\langle \bar{\mathbf{u}} \rangle \langle \bar{T} \rangle) = \nabla \cdot \mathbf{K}_{eff} \cdot \nabla \langle \bar{T} \rangle \tag{17}$$

where $\langle j_b \rangle$ is the volume average of j_b, $\langle j_b \rangle^b$ the intrinsic average of j_b in the b phase, j'_b the time fluctuation of j_b, ${}^i j_b$ the space deviation of j_b, f_f the volume fraction of fluid and $f_s = 1 - f_f$ the volume fraction of solid. The effective conductivity, $\mathbf{K}_{eff}$, the tortuosity tensor, $\mathbf{K}_{tor}$, and the dispersion tensor, $\mathbf{K}_{dis}$, are defined as:

$$\mathbf{K}_{eff} = (f_f \frac{\rho_f c_{pf} \nu_{t_f}}{\sigma_t} + f_f k_f + f_s k_s)\mathbf{I} + \mathbf{K}_{tor} + \mathbf{K}_{dis} \tag{18}$$

$$\mathbf{K}_{tor} \cdot \nabla \langle \overline{T} \rangle = \frac{(k_f - k_s)}{\Delta V} \int_{A_i} \mathbf{n}_f \, {}^i\overline{T}_f \, dS \tag{19}$$

$$\mathbf{K}_{dis} \cdot \nabla \langle \overline{T} \rangle = -r_f c_{pf} f_f \langle {}^i\overline{\mathbf{u}} \, {}^i\overline{T}_f \rangle^f = -\frac{r_f c_{pf}}{\Delta V} \int_{\Delta V_f} {}^i\overline{\mathbf{u}} \, {}^i\overline{T}_f \, dV \tag{20}$$

Pedras *et al.* (2003b) and Pedras *et al.* (2004) utilized Eq. (20) for calculating the diagonal components of $\mathbf{K}_{dis}$ in an infinite porous medium formed by a spatially periodic array of longitudinally-displaced elliptic rods (Fig. 2a) and by a spatially periodic array of transversally-displaced elliptic rods (Fig. 2b), respectively. In both cases the authors utilized two types of boundary conditions for the temperature, the Dirichlet boundary conditions:

$$\overline{T}_{x=0} = \overline{T}_{x=H} - \Delta \langle \overline{T} \rangle_x \text{ and } \overline{T}_{y=0} = \overline{T}_{y=H} \tag{21}$$

for the longitudinal thermal dispersion, $(K_{dis})_{xx}$, calculation, and,

$$\overline{T}_{x=0} = \overline{T}_{x=H} \text{ and } \overline{T}_{y=0} = \overline{T}_{y=H} - \Delta \langle \overline{T} \rangle_y \tag{22}$$

for the transverse thermal dispersion, $(K_{dis})_{yy}$, calculation. And the Neumann boundary conditions, Fig (3a) for the $(K_{dis})_{xx}$ calculation and Fig (3b) for the $(K_{dis})_{yy}$ calculation.

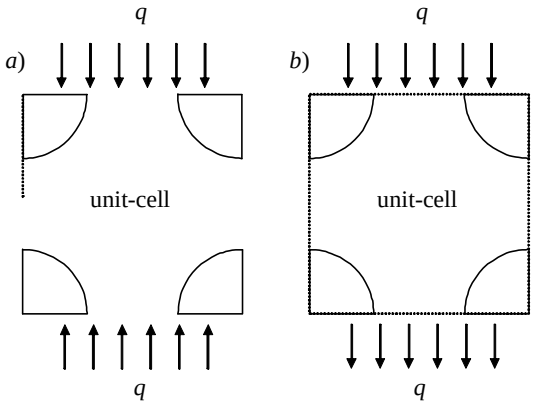

Figure 3. Neumann Boundary conditions for the temperature $k_f \frac{\partial \overline{T}}{\partial y} = k_s \frac{\partial \overline{T}}{\partial y} = -q$.

4. Numerical Model

The governing equations were discretized using the finite volume procedure, Patankar (1980). The SIMPLE algorithm for the pressure-velocity coupling was adopted to correct both the pressure and the velocity fields. The process starts with the solution of the two momentum equations. Then the velocity field is adjusted in order to satisfy the continuity principle. This adjustment is obtained by solving the pressure correction equation. After that, the turbulence model equations and the energy equation are relaxed to update the *k*, *e* and temperature fields. Details on the numerical discretization and procedure can be found in Pedras and de Lemos (2001b), Pedras *et al.* (2003b) and Pedras *et al.* (2004).

5. Results and Discussion

A total of twenty seven runs, for each case, were carried out with a fluid phase Prandtl number of 0.72 and a thermal conductivity ratio, k_s/k_f , between the solid and fluid phase of 2. Values for $(K_{dis})_{xx}$ and $(K_{dis})_{yy}$ were obtained varying the $\mathrm{Pe}_H = |\langle \overline{\mathbf{u}} \rangle| H / a_f$ from 10^0 to 4.10^3 and the $f_f = 1 - ab\pi/H^2$, from 0.60 to 0.90.

The longitudinal components of the thermal dispersion tensor for the two porous media are shown in Fig. (4) as a function of Peclet number and for different porosities. In the Fig. (4a) the thermal dispersion calculation was carried out with Neumann boundary conditions for the temperature (Fig. 3a), while Fig (4b) was carried out with Dirichlet boundary conditions (Eq. 21). For the longitudinal ellipses its overall dependence on the Peclet number was $(K_{dis})_{xx}/k_f = 3.52\times10^{-2}\,\mathrm{Pe}_H{}^{1.65}$, including Neumann and Dirichlet boundary conditions. While for the transverse ellipses its overall dependence was $(K_{dis})_{xx}/k_f = 4.74\times10^{-2}\,\mathrm{Pe}_H{}^{1.65}$, showing, in both cases, the usual behavior of ($\sim \mathrm{Pe}_H{}^n$) as expected. The power dependence on the Peclet number of about 1.65 was lower than the square dependence of Taylor dispersion in a tube. This behavior can be ascribed to the turbulence, which contributes to the enhancement of the transverse dispersion. The results of Quintard *et al.* (1997) show a dependence of about 1.3 for a staggered arrangement of cylinders and spheres and 1.7 for in-line arrangement. Their work was restricted to Stokes' flow and the value of 1.3 was ascribed to the enhancement of the transverse dispersion in the staggered arrangement.

As previously mentioned, these distinct morphologies produce large different pressure drops (Pedras and de Lemos, 2003), however, for the longitudinal component of the thermal dispersion tensor this not occur, they have almost the same results. A possible explanation is that in both cases mass flow rate imposed were the same (producing identical Peclet numbers), *i.e.*, they have the same thermal convection in the longitudinal direction.

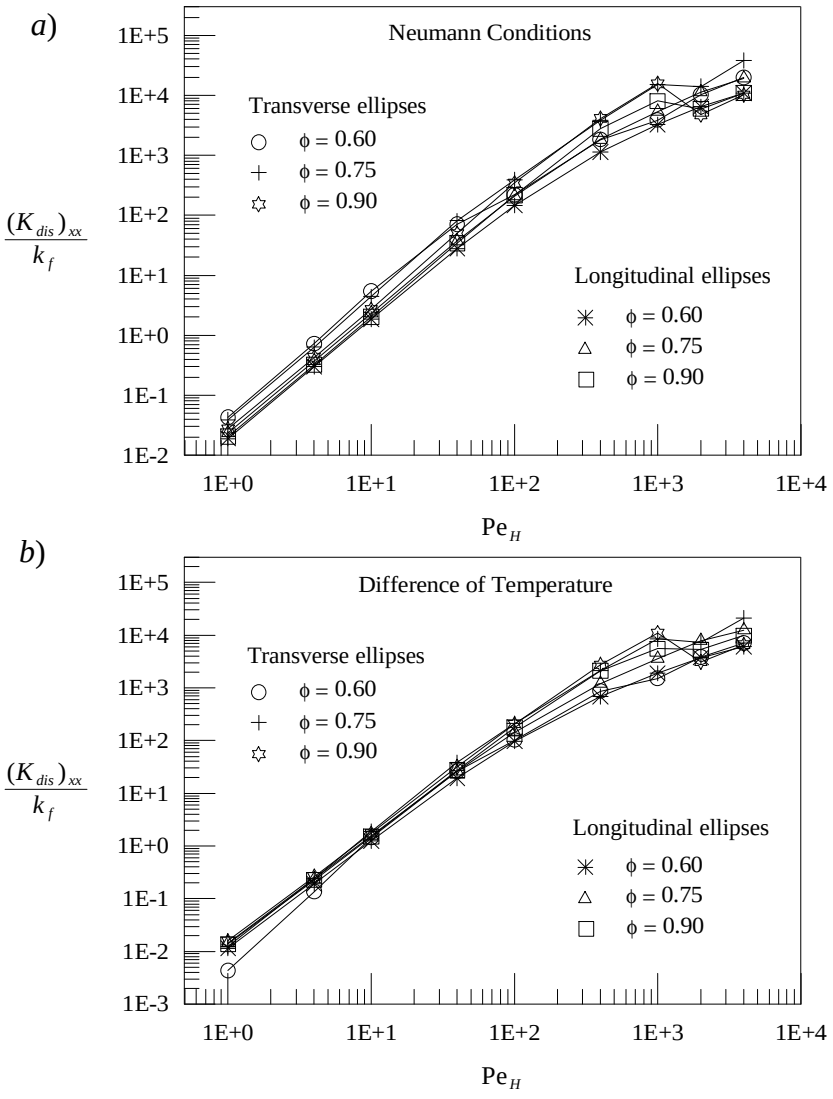

Figure 4. Longitudinal thermal dispersion comparing: *a*) using Neumann Boundary conditions (Fig. 3a) *b*) using Dirichlet Boundary conditions (Eq. 21).

The transverse components of the thermal dispersion tensor for the two porous media are shown in Fig. (5) as a function of Peclet number and for different porosities. In the Fig. (5a) the thermal dispersion calculation was carried out with Neumann boundary conditions for the temperature (Fig. 3b), while Fig (5b) was carried out with Dirichlet boundary conditions (Eq. 22). For the longitudinal ellipses its overall dependence on the Peclet number was $(K_{dis})_{yy}/k_f = 2.29\times10^{-4}\mathrm{Pe}_H{}^{0.88}$, including Neumann and Dirichlet boundary conditions. While for the transverse ellipses its overall dependence was $(K_{dis})_{yy}/k_f = 1.43\times10^{-3}\mathrm{Pe}_H{}^{1.05}$. As expected, in both cases their transverse components are much smaller than their longitudinal component for large Peclet numbers.

Differently from the longitudinal components, the values of the transverse components differ greatly between the longitudinal ellipses and transverse ellipses. This can be explained by the fact that in the transverse direction the change in the morphology provides different convective heat transfer between the north and south faces of the unit-cell. The transverse ellipses provided greater convective heat transfer in the transverse direction than the longitudinal ellipses.

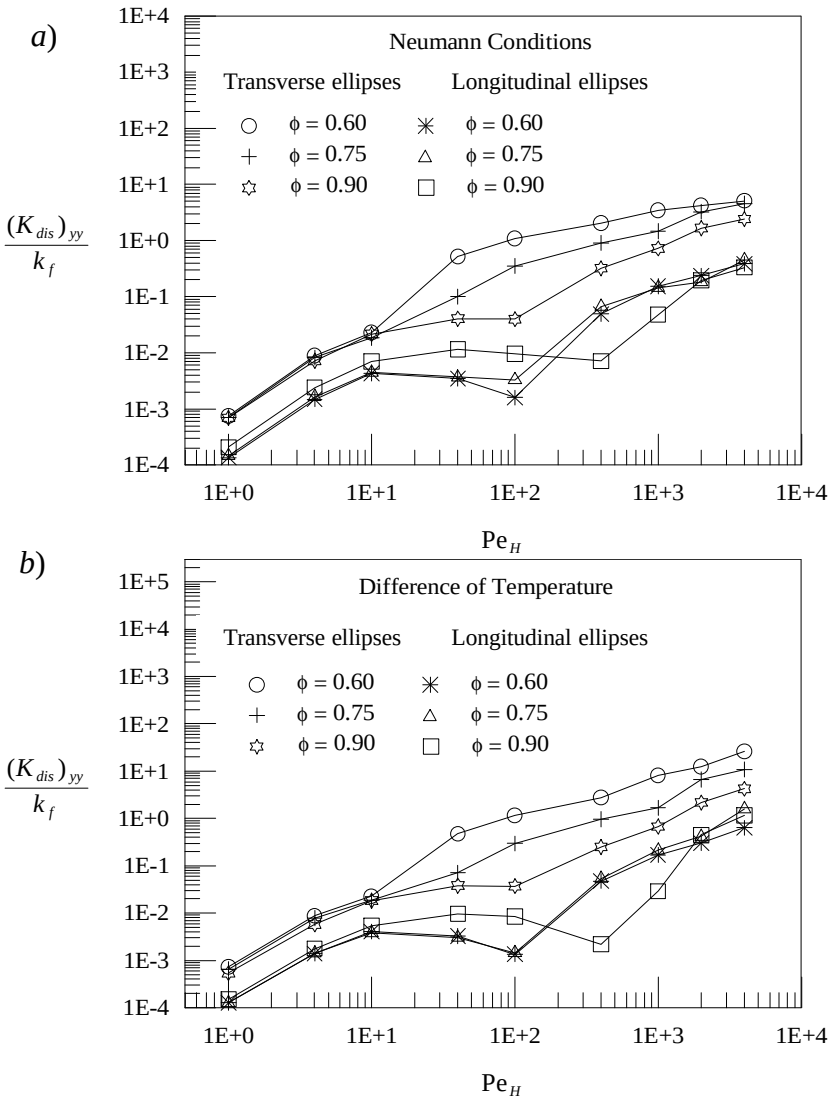

Figure 5. Transverse thermal dispersion comparing: *a*) using Neumann Boundary conditions (Fig. 3b) *b*) using Dirichlet Boundary conditions (Eq. 22).

6. Conclusions

Results of thermal dispersion components calculated for a periodic porous medium represented by a unit-cell with Neumann and Dirichlet boundary conditions for the energy equation and periodic boundary condition for mass and momentum equations were presented for two distinct porous medium morphologies and compared among them. The longitudinal components of the thermal dispersion show little variation with the morphology of the medium, while the transverse components show great variation.

7. Acknowledgements

The authors are thankful to FAPESP and CNPq, for their financial support during the course of this research.

8. References

Abe, K., Nagano, Y., and Kondoh, T., 1992, An Improved k-ε Model for Prediction of Turbulent Flows with Separation and Reattachment, Trans. JSME, Ser. B, vol. 58, pp. 3003-3010.

de Lemos, M.J.S. and Pedras, M.H.J., 2001, Recent Mathematical Models for Turbulent Flow in Saturated Rigid Porous Media, ASME Journal of Fluids Engineering, vol. 123 (4), pp. 935-940.

Hsu, C. T. and Cheng, P., 1990, Thermal Dispersion in a Porous Medium, Int. J. Heat Mass Transfer, vol. 33, pp. 1587-1597.

Kaviany, M., 1995, *Principles of Heat Transfer in Porous Media*, 2nd edn. Springer, New York.

Kuwahara, F. and Nakayama, A., 1998, Numerical Modeling of Non-Darcy Convective Flow in Porous Medium, Proc. of 11th IHTC (Kyongju, Korea), vol. 4, pp. 411-416.

Launder, B.E. and Spalding, D.B., 1974, The numerical computation of turbulent flows, Comp. Meth. Appl. Mech. Eng., vol. 3, pp. 269-289.

Moyne, C., 1997, Two-Equation Model for a Diffusive Process in Porous Media Using the Volume Averaging Method with an Unsteady-State Closure, Adv. Water Resour., vol. 20 (2-3), pp. 63-76.

Nakayama, A. and Kuwahara, F., 1999, A Macroscopic Turbulence Model for Flow in a Porous Medium, ASME Journal of Fluids Engineering, vol. 121, pp. 427-433.

Ochoa-Tapia, J. A. and Whitaker, S., 1997, Heat Transfer at the Boundary Between a Porous Medium and a Homogeneous Fluid, Int. J. Heat Mass Transfer, vol. 40 (11), pp. 2691-2707.

Patankar, S. V., 1980, *Numerical Heat Transfer and Fluid Flow*, Hemisphere, New York.

Pedras, M.H.J. and de Lemos, M.J.S., 2001a, Macroscopic Turbulence Modeling for Incompressible Flow Through Undeformable Porous Media, Int. J. Heat Mass Transfer, vol. 44 (6), pp. 1081-1093.

Pedras, M.H.J. and de Lemos, M.J.S., 2001b, Simulation of Turbulent Flow in Porous Media Using a Spatially Periodic Array and a Low Re Two-Equation Closure, Numer. Heat Transfer, Part A-Appl, vol. 39 (1), pp. 35-59.

Pedras, M.H.J. and de Lemos, M.J.S., 2001c, On Mathematical Description and Simulation of Turbulent Flow in a Porous Medium Formed by an Array of Elliptic Rods, ASME Journal of Fluids Engineering, vol. 123 (4), pp. 941-947.

Pedras, M.H.J. and de Lemos, M.J.S., 2003, Computation of Turbulent Flow in Porous Media Using a Low Reynolds *k-e* Model and an Infinite Array of Transversally Displaced Elliptic Rods, Numer. Heat Transfer; Part A-Appl. vol. 43, n. 6, pp. 585-602.

Pedras, M.H.J., Rocamora, F.D. and de Lemos, M.J.S., 2003a, Simulation of Turbulent Thermal Dispersion in Porous Media Using a Periodic Cell with Prescribed Heat Flux at the Boundaries, Proc. of 3rd Int. Conf.. Computational Heat and Mass Trans., May 26-30, Banff, Canada.

Pedras, M.H.J., Rocamora, F.D. and de Lemos, M.J.S., 2003b, Turbulent Dispersion in a Porous Media Modeled as an Infinite Array of Longitudinally-Displaced Elliptic Rods, *Proc. of COBEM2003 17th International Congress of Mechanical Engineering*, November 10-14, São Paulo, Brasil.

Pedras, M.H.J. and de Lemos, M.J.S., 2004, Turbulent Dispersion in Porous Media Modeled as an Infinite Array of Transversally-Displaced Elliptic Rods, *Proc. of APM2004 2nd International Conference on Applications of Porous Media*, May 24-27, Evora, Portugal.

Quintard, M., Kaviany, M. and Whitaker, S., 1997, Two-Medium Treatment of Heat Transfer in Porous Media: Numerical Results for Effective Proprieties, Adv. Water Resour., vol. 20 (2-3), pp. 77-94.

Rocamora, F.D. and de Lemos, M.J.S., 2000, Analysis of Convective Heat Transfer for Turbulent Flow in Saturated Porous Media, Intern. Comm. Heat and Mass Transfer, vol. 27 (6), pp. 825-834.

Rocamora, F.D., de Lemos M.J.S. 2002, Numerical Determination Of The Thermal Dispersion Tensor In An Infinite Porous Medium, *Numerical Heat Transfer* (submitted).

9. Copyright Notice